

Model Predictive Current Control with Neutral Current Elimination for H-Bridge Two-Level Active Power Filters

A. Renault*, M. Rivera[†], L. Comparatore*, J. Pacher*, J. Rodas* and R. Gregor*

*Laboratory of Power and Control Systems, Facultad de Ingeniería, Universidad Nacional de Asunción

E-mail: {arenault, lcomparatore, jpacher, jrodas, rgregor }@ing.una.py

[†]Department of Industrial Technologies, Universidad de Talca

E-mail: marcoriv@utalca.cl

Abstract—In this paper, a scheme for reactive power compensation and neutral current elimination based on model predictive control strategy is proposed. In this context, a H-bridge four-wire two-level active power filter is presented. The main feature of the proposed method focuses on the compensation of reactive power and neutral current elimination for unbalanced load in order to improve the power factor. This approach predicts the future behavior of the control actions considering all possible switching states. The proposed method selects the optimal switching vector by using an optimization process considering a defined cost function. The effectiveness of the proposed control approach is evaluated through simulations.

Index Terms—Active power filters, H-bridge converter, predictive current control, neutral current elimination.

I. INTRODUCTION

In the last decades, the use of electronic-based power loads increased greatly and consequently the contamination of the distribution systems. In order to solve the various problems of power quality in distribution systems, active power filters (APF) and multilevel static synchronous compensators (M-STATCOM) are considered one of the best and the most popular solution [1]. The purpose of using a four-wire APF, is to perform the suppression of harmonic current, reactive power compensation, power factor correction and neutral current elimination [2], [3]. This can be achieved by the injection of currents at the point of common coupling (PCC) [4]. This type of APF usually requires four H-bridge voltage source inverters (VSI) which provides neutral current through the fourth H-bridge [5], or three H-bridge VSI with star configuration and accessible neutral-wire [6].

As main contribution, and complementing previous works, i.e. [7], a method for power compensation and neutral current elimination applied to a three-phase four-wire H-bridge two-level APF is proposed by using predictive current control. Predictive model is obtained from the dynamic equations of the compensation system. Simulation results have been analyzed in order to verify the effectiveness of the proposed method.

This paper is organized as follows: Section II describes the three-phase four-wire H-bridge APF topology. Section III discusses the proposed model-based predictive control (MPC) strategy. Section IV discusses the effectiveness of the proposed

method considering the simulation results. Finally, concluding remarks are summarized in Section V.

II. THREE-PHASE FOUR-WIRE H-BRIDGE APF TOPOLOGY

Fig. 1 shows the proposed three-phase four-wire two-level H-bridge APF topology, consisting in one H-bridge cells per phase. The different H-bridge cells have an independent DC-link (C_{dc}). Each cell contains four switching devices, resulting in a total of 16 power switchers. Consequently, four switching signals (S_{fij}) are needed in order to controlled each cell, where f represents the phase (a, b, c and n), i the cell number in the corresponding phase (1, 2, 3 or 4) and j the switching device corresponding to the cell (1, 2, 3 or 4), respectively.

Table I shows the allowed combinations of activation signals and the respective output voltages corresponding to the Cell₁ of the phase “a”, where v_{dc} is the voltage of the capacitor. Similar allowed combinations are defined for the other cells. Other possible combinations are not permitted because they cause a short circuit in the DC-link of the cell. To avoid this, only two activation signals and they complementary levels are used as shown in Fig. 1 for the particular case of Cell₁.

A. Two-level H-bridge APF model

The dynamic model of the circuit configuration (Fig. 2) can be obtained by using Kirchhoff’s circuit laws. For modeling purposes, it is assumed that the three-phase voltage sources are balanced and all modules have the same capacitance and voltage in their DC side. The two-level H-bridge APF is connected at the PCC. Applying Kirchhoff’s voltage law for the AC side of the APF, the following equations are obtained:

$$\frac{di_c^{abcn}}{dt} = \frac{v_s^{abcn}}{L_f} - \frac{R_f}{L_f} i_c^{abcn} - \frac{n_c S_{fij} v_{dc}^{abcn}}{L_f} \quad (1)$$

$$\frac{dv_{dc}^{abcn}}{dt} = \frac{S_{fij} i_c^{abcn}}{C_{dc}} - \frac{v_{dc}^{abcn}}{R_{dc} C_{dc}} \quad (2)$$

where n_c is the number of cells, R_{dc} is a resistor connected in parallel to the capacitor C_{dc} that concentrates the overall losses in the DC side, S_{fij} is the commutation function and the resistor R_f is the parasitic (series) resistance of the inductor L_f .

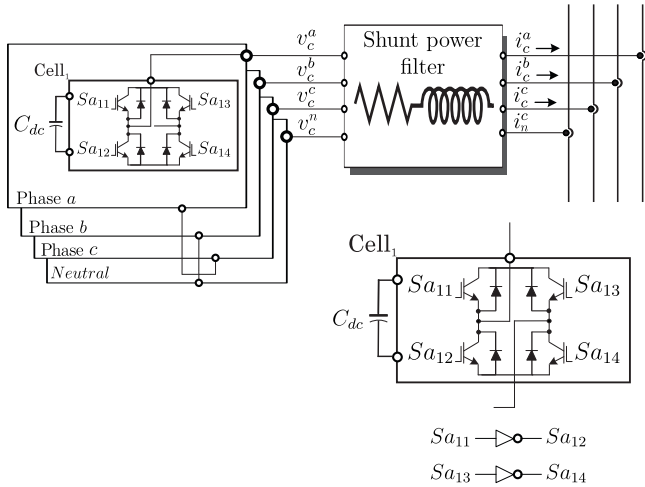


Fig. 1. Three-phase four-wire two-level H-bridge APF.

TABLE I
ALLOWED COMBINATIONS OF ACTIVATION SIGNALS

Sa_{11}	Sa_{13}	Sa_{12}	Sa_{14}	v_c^a
1	0	0	1	$+v_{dc}$
1	1	0	0	0
0	0	1	1	0
0	1	1	0	$-v_{dc}$

III. PREDICTIVE CONTROL STRATEGY

For two-level H-bridge APFs, the differential equation that models the AC side is [8], [9]:

$$\frac{di_c^{abcn}}{dt} = \frac{v_s^{abcn}}{L_f} - \frac{v_c^{abcn}}{L_f} - \frac{R_f i_c^{abcn}}{L_f} \quad (3)$$

The predictive model can be obtained by using a forward Euler discretization method from the continuous time-domain model represented by (3), which yields to the following equation:

$$i_c^{abcn}(k+1) = \left(1 - \frac{R_f T_s}{L_f}\right) i_c^{abcn}(k) + \frac{T_s}{L_f} \{v_s^{abcn}(k) - v_c^{abcn}(k)\} \quad (4)$$

where k identifies the actual discrete-time sample, T_s is the sampling time, and $i_c^{abcn}(k+1)$ are a prediction of the APF phase currents made at sample k .

Fig. 3 shows the proposed scheme of the predictive current control technique applied to the three-phase four-wire two-level H-bridge APF system. In the proposed control the predicted errors are computed for each possible voltage vector as:

$$e_{i_c}^{abcn}(k+1) = i_c^{abcn*}(k+1) - i_c^{abcn}(k+1) \quad (5)$$

being e_{i_c} the APF current errors in the AC side, respectively. For each of them a cost function is evaluated. The cost function has been typically defined as a quadratic measure of the predicted error, which can be defined as [7]:

$$J(k+1) = \|e_{i_c}^{abcn}(k+1)\|^2 \quad (6)$$

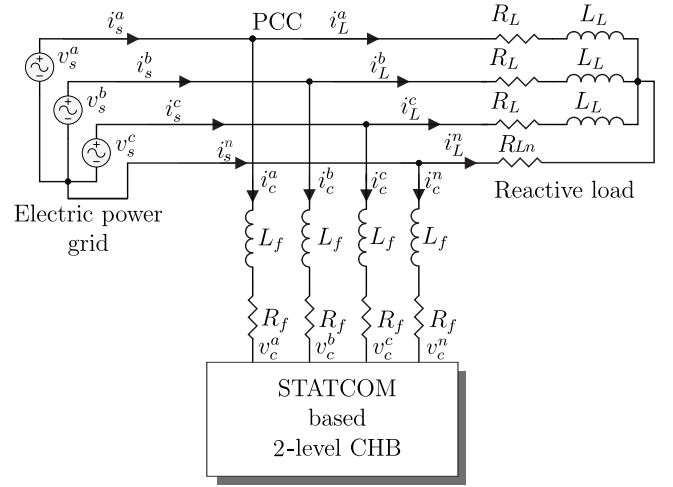


Fig. 2. Two-level H-bridge APF connection.

A. Reference generation

The instantaneous active and reactive power references are obtained from the Clarke transformation approach in $\alpha - \beta - 0$ reference frame by using the following transformation matrix:

$$\mathbf{T} = \sqrt{\frac{2}{3}} \begin{bmatrix} 1 & -\frac{1}{2} & -\frac{1}{2} \\ 0 & \frac{\sqrt{3}}{2} & -\frac{\sqrt{3}}{2} \\ \frac{1}{\sqrt{2}} & \frac{1}{\sqrt{2}} & \frac{1}{\sqrt{2}} \end{bmatrix} \quad (7)$$

Applying (7), the $\alpha - \beta - 0$ current references in the AC side of the APF are obtained from [10]:

$$\begin{bmatrix} i_{c\alpha}^* \\ i_{c\beta}^* \end{bmatrix} = \frac{1}{(v_{s\alpha})^2 + (v_{s\beta})^2} \begin{bmatrix} v_{s\alpha} & v_{s\beta} \\ v_{s\beta} & -v_{s\alpha} \end{bmatrix} \begin{bmatrix} P_c^* \\ Q_c^* \end{bmatrix} \quad (8)$$

and i_{c0}^* simplified is:

$$i_{c0}^* = i_{L0} \quad (9)$$

where the superscript (*) denotes the reference variables and P_c^* , Q_c^* are the instantaneous active and reactive power references and the P_{c0}^* is the zero sequence instantaneous power, respectively. In order to allow a unitary power factor at the grid side and considering which ideally the APF do not absorb any active power, the instantaneous power references can be written as [11]:

$$P_c^* = 0 \quad (10)$$

$$Q_c^* = -Q_L = v_{s\alpha} i_{L\beta} - v_{s\beta} i_{L\alpha} \quad (11)$$

$$P_{c0}^* = -P_{L0} = -i_{L0} v_{s0} \quad (12)$$

being Q_L the instantaneous reactive and P_{L0} is the zero sequence instantaneous power, in the load power to be compensate by the two-level H-bridge APF system. The STATCOM phase currents references used in the optimization process are:

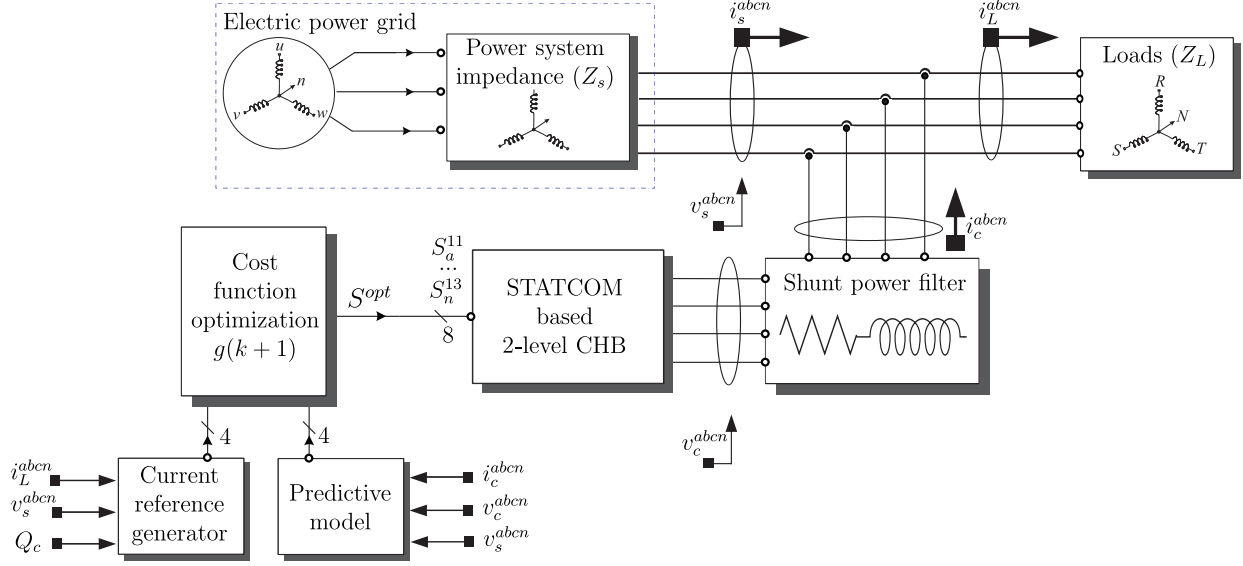


Fig. 3. Block diagram of the proposed control scheme.

$$i_c^{abc*} = \mathbf{T}^{-1} [i_{c\alpha}^* \quad i_{c\beta}^* \quad i_{c0}^*]' \quad (13)$$

where the superscript (') indicates the transposed matrix.

B. Optimization process

The optimization is performed by exhaustive search over all possible switching vectors of the control action. If n is the number of H-bridge cells per phase (f), then each vector S_{fij} consists in $2n$ choice signals, where $j = 1, \dots, \phi$; being ϕ the number of phases. Moreover, the number of possible switching vectors per phase can be defined as $\varepsilon = 2^{2n}$. During the optimization process, both, the cost function and the predictive model must be computed 4 times at each sampling period to guarantee optimality, since there are 4 possible switching vectors for the case study. These switching vectors represent all possible output voltages of the STATCOM, v_c^a , v_c^b , v_c^c and v_c^n , connected at the PCC point. The output voltages can be represented by the following equation:

$$\begin{bmatrix} v_c^a \\ v_c^b \\ v_c^c \\ v_c^n \end{bmatrix} = \begin{bmatrix} v_{c1} \\ v_{c2} \\ v_{c3} \\ v_{c4} \end{bmatrix} v_{dc} \quad (14)$$

where v_{c1} , v_{c2} , v_{c3} and v_{c4} are the optimal levels of the three-phase four-wire two-level H-bridge APF system $(-1, 0, 1)$.

IV. SIMULATION RESULTS

The proposed control strategy was simulated using MATLAB/Simulink considering 40 kHz of sampling frequency and 342 V of the DC side [12]. The electrical parameters as well as the MPC parameters are shown in Table II. Numerical integration using Runge-Kutta method has been applied to compute the evolution of the variables step by step in the time-domain.

Algorithm 1 Optimization algorithm

1. Initialize $J_o^a := \infty, J_o^b := \infty, J_o^c := \infty, J_o^n := \infty, \eta := 0$
2. Compute the STATCOM reference currents. Eqn. (13)
3. **while** $\eta \leq \varepsilon$ **do**
4. $S_{fij} \leftarrow S_{fij}^\eta \quad \forall i = 1, 2, 3, 4 \ \& \ j = 1, 2, 3, 4$
5. Compute the STATCOM prediction currents. Eqn. (4)
6. Compute the errors. Eqn. (5)
7. Compute the cost function. Eqn. (6)
8. **if** $J^a < J_o^a$ **then**
9. $J_o^a \leftarrow J^a, S_a^{opt} \leftarrow S_{a_{ij}}$
10. **end if**
11. **if** $J^b < J_o^b$ **then**
12. $J_o^b \leftarrow J^b, S_b^{opt} \leftarrow S_{b_{ij}}$
13. **end if**
14. **if** $J^c < J_o^c$ **then**
15. $J_o^c \leftarrow J^c, S_c^{opt} \leftarrow S_{c_{ij}}$
16. **end if**
17. **if** $J^n < J_o^n$ **then**
18. $J_o^n \leftarrow J^n, S_n^{opt} \leftarrow S_{n_{ij}}$
19. **end if**
20. $\eta := \eta + 1$
21. **end while**

Fig. 4 (upper) shows the active and reactive power on the grid side. The active power remains constant load balanced, when the unbalance occurs to 0.04 s, oscillates due to impedance variations and current circulating in the load. While the reactive power is maintained in the near average zero before and after the load unbalance. In Fig. 4 (bottom) i_c^a , i_L^a and i_s^a currents are observed, respectively.

On the hand Fig. 5 system behavior in balanced load is observed during the first 0.04 s. At that moment the load is changed in the phase "a", which makes the load is unbalanced. The dynamics of the system tracks the reference current i_c^{a*} ,

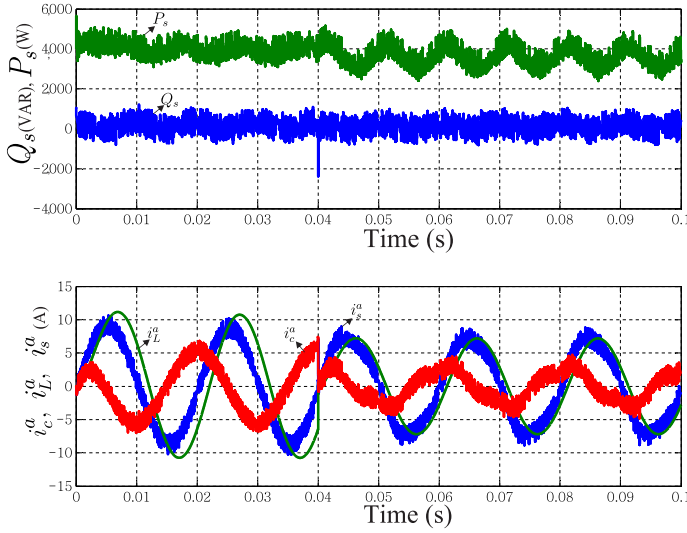


Fig. 4. Two-level H-bridge APF transient response, active and reactive power compensation.

TABLE II
PARAMETERS DESCRIPTION

PARAMETER	Two-Level CHB STATCOM		
	SYMBOL	VALUE	UNIT
Electric frequency of the grid	f_e	50	Hz
Voltage of the electric grid	v_s	310,2	V
Filter resistance	R_f	0,09	Ω
Filter inductance	L_f	3	mH
DC-link voltage	v_{dc}	342	V
Load parameters			
Load resistance	R_L	23,2	Ω
Neutral load resistance	R_{Ln}	1	Ω
Change load	R_L	40	Ω
Load inductance	L_L	55	mH
Predictive control parameters			
Sampling time	T_s	25	μs
Active power reference	P_c^*	0	W
Ideal Reactive power reference	Q_c^*	$-Q_L$	VAR
Zero sequence instantaneous power	P_{c0}^*	$-PL_0$	W

even if the load imbalance occurs, the system has performed well by injecting reactive power.

Then, in Fig. 6 the current in phase "a" of the APF, i_c^a and i_c^{a*} to unbalance load occur, as current monitoring occurs. Moreover, Fig. 7 system dynamics is observed in the neutral charge i_L^n , as the injected current i_c^n and reference i_c^{n*} STATCOM. Even at 0.04 s. the system has load balancing and load current i_L^n is zero, the neutral current injected by the APF. When the load unbalance occurs, the current injected by the APF and the neutral current of the load 180 degrees so that compensate. It can be observed that the neutral current of the i_s^n source it is on average approximately zero, which meets the parameters of calculation and design of active filter.

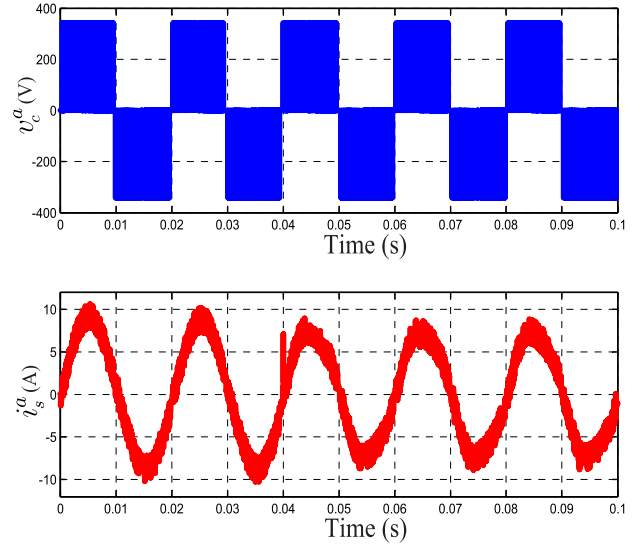


Fig. 5. Dynamic response evolution of v_c^a , i_s^a and current tracking considering a reactive power step with a load change in the phase "a".

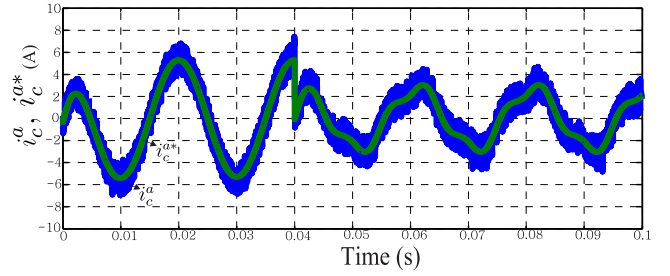


Fig. 6. Dynamic response evolution of i_c^a , i_c^{a*} and current tracking considering a reactive power step with a load change in the phase "a".

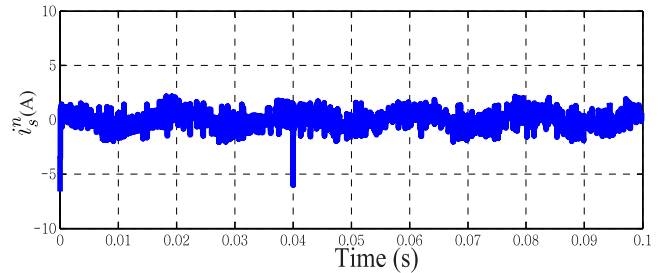
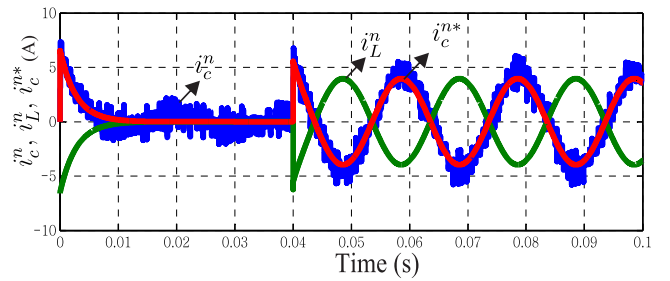


Fig. 7. Dynamic response evolution of i_c^n , i_c^{n*} and i_L^n neutral current in the load and injection current compensating filter neutral load with a load change in the phase "a".

V. CONCLUSION

In this paper, a predictive current control technique for a two-level H-bridge APF has been proposed and analyzed. It has been shown that it is possible to compensate the reactive power and instantaneous neutral current in unbalanced load for improving the power factor of the mains. The simulation results confirm the ability of the proposed technique in the field of instantaneous reactive power compensation and neutral current for unbalanced load.

ACKNOWLEDGMENT

The authors would like to acknowledge the financial support of FONDECYT Regular 1160690 project and Paraguayan Government support provided by means of a CONACYT project 14-INV-096.

REFERENCES

- [1] S. A. Kamran and J. Muñoz, "Study of a state-of-the art M-STATCOM," in *Proc. ICIT*, 2015, pp. 2733–2738.
- [2] M. Kumar and M. Mishra, "Three-leg inverter-based distribution static compensator topology for compensating unbalanced and non-linear loads," *IET Power Electron.*, vol. 8, no. 11, pp. 2076–2084, 2015.
- [3] A. K. Balasubramanian and V. John, "Thermal test method for high power three-phase grid-connected inverters," *IET Power Electron.*, vol. 8, no. 9, pp. 1670–1680, 2015.
- [4] G. Buticchi, D. Barater, C. Concari, and G. Franceschini, "Single-phase series active power filter with transformer-coupled matrix converter," *IET Power Electron.*, vol. 9, no. 6, pp. 1279–1289, 2016.
- [5] E. Fabricio, C. Jacobina, and V. Nobrega, "Four-wire shunt compensator based on H-bridge Y-connected converters," in *Proc. IECON*, 2014, pp. 5184–5190.
- [6] H. Huang, R. Xu, and H. Wang, "The study of three-phase four-wire shunt active power filter," in *Proc. MEC*, 2013, pp. 3496–3499.
- [7] R. Gregor, L. Comparatore, A. Renault, J. Pacher, J. Rodas, S. Toledo, and M. Rivera, "A novel predictive-fixed switching frequency technique for a cascade H-Bridge multilevel STATCOM," in *Proc. IECON*, 2016.
- [8] S. Mikkili and A. K. Panda, "Power quality issues and solutions—review," *Int. J. Emerg. Elec. Power Syst.*, vol. 16, no. 4, pp. 357–384, 2015.
- [9] A. Hamidi, A. Ahmadi, M. S. Feali, and S. Karimi, "Implementation of digital FCS-MP controller for a three-phase inverter," *Electr. Eng.*, vol. 97, no. 1, pp. 25–34, 2015.
- [10] A. K. Panda and R. Patel, "Adaptive hysteresis and fuzzy logic controlled-based shunt active power filter resistant to shoot-through phenomenon," *IET Power Electron.*, vol. 8, no. 10, pp. 1963–1977, 2015.
- [11] L. B. G. Campanhol, S. A. O. da Silva, and A. Goedel, "Application of shunt active power filter for harmonic reduction and reactive power compensation in three-phase four-wire systems," *IET Power Electron.*, vol. 7, no. 11, pp. 2825–2836, 2014.
- [12] Y. Li, Z. Ye, N. He, J. Wu, C. Hu, and D. Xu, "Efficiency improvement of a SiC-MOSFET 500 kHz ZVS inverter," in *Proc. PEDG*, 2016, pp. 1–8.